Iterative ADMIRE for High Dynamic Range B-mode

Siegfried Schlunk

Department of Biomedical Engineering Department of Biomedical Engineering Department of Biomedical Engineering Vanderbilt University Nashville, TN, USA siegfried.g.schlunk@vanderbilt.edu

Kazuyuki Dei

Vanderbilt University Nashville, TN, USA

Brett Byram

Vanderbilt University Nashville, TN, USA

Abstract—Some adaptive beamformers struggle with high dynamic range scenarios, as notably demonstrated by the dark region artifact (DRA), which can appear when these beamformers are applied in the proximity of strong acoustic sources. The DRA is detrimental because it may mask important features that are weaker acoustically. In a previous study, we used our aperture domain model image reconstruction algorithm (ADMIRE) that was able to partially mitigate the DRA and had improved dynamic range compared to other common beamformers. Here, we introduce an iterative variant of ADMIRE (iADMIRE) that is more fully able to remove the DRA and preserve speckle texture, while also having increased dynamic range. We compared iAD-MIRE to traditional DAS, DMAS, GCF, and normal ADMIRE. iADMIRE demonstrated the highest dynamic range of 69.6 dB, an increase of 19.2 dB compared to DAS and 20.3 dB compared to ADMIRE, and fully restored speckle texture in regions near bright targets up to 100 dB.

Index Terms—ADMIRE, iterative, dynamic range, dark region

I. INTRODUCTION

We previously introduced contrast ratio dynamic range as a new beamformer performance metric, where several adaptive beamformers were compared [1]. As was shown, several of these beamformers struggle to achieve a high dynamic range compared to delay-and-sum (DAS). For scenarios with multiple high dynamic range features, this can result in saturation, where different targets may incorrectly appear to be at the same acoustic strength.

At the same time, another group published a report on the dark region artifact (DRA), which is characterized as a dark region near a bright, or strong, acoustic target [2]. This artifact is suggested to arise from a failure to differentiate mainlobe versus sidelobe signals, and may as a results mask important features that are weaker acoustically. We expect that this artifact could appear in vivo in proximity to strong acoustic targets such as kidney stones or near the lungs, though this has yet to be tested.

In a previous paper, our aperture domain model image reconstruction (ADMIRE) [3], [4], [5] was able to reduce the severity of the DRA, but not remove it completely [6]. Here, we introduce an iterative version of this method (iADMIRE), that is able to achieve higher dynamic range and remove the artifact more effectively. We compare these two methods to DAS, delay multiply and sum (DMAS) [7], and generalized coherence factor (GCF) [8].

II. BEAMFORMING ALGORITHMS

A. Delay-and-Sum (DAS)

Conventional delay-and-sum (DAS) involves dynamically delaying the received channel data such that focusing is achieved at all depths and all lateral locations. The data for each line is then summed along the channel dimension, producing a complete image.

B. Delay Multiply and Sum (DMAS)

Delay multiply and sum (DMAS) is an extension of DAS where the delayed channel data is combinatorically coupled and multiplied prior to summation [7]. The DMAS signal at depth k is calculated as

$$s_{DMAS}^* = \sum_{i=1}^{M-1} \sum_{j=i+1}^{M} \hat{s}_{ij}(k), \tag{1}$$

where M is the number of channels, and $\hat{s}_{ij}(k)$ is further defined

$$\hat{s}_{ij}(k) = sign(s_i(k)s_j(k))\sqrt{|s_i(k)s_j(k)|}, \qquad (2)$$

where $s_i(k)$ is the signal for channel i. The DC and high frequency components are then removed from the DMAS signal with a band-pass filter around $2f_c$.

C. Generalized Coherence Factor (GCF)

Generalized coherence factor (GCF) is an extension of coherence factor (CF), where the DAS image is weighted by the ratio of energy in some low-frequency region across the aperture to the total energy [8]. This ratio for a depth k is defined as

$$GCF(k) = \frac{\sum_{k=0}^{M_0} |p(k)|^2}{\sum_{k=0}^{M} |p(k)|^2},$$
 (3)

where p(k) is the M-point discrete Fourier transform across the aperture, and M_0 is the chosen cutoff frequency index for the low-frequency region. In this paper, we choose M_0 = 5. The GCF image is then obtained by simply element-wise multiplying the GCF and the DAS image.

D. Aperture Domain Model Image Reconstruction (ADMIRE)

The aperture domain model image reconstruction (AD-MIRE) algorithm was developed primarily to detect and remove reverberation, off-axis clutter, and wavefront aberration, and is explained elsewhere in detail [3], [4], [5]. The foundation of ADMIRE is the well-defined physics of linear wave propagation, from which a model of the effects of scatterers and reverberant sources can be created. Concisely, this model allows us to breakdown a given wavefront into its sources of origin, whereby we can reject any signal originating from outside our region of interest. Here, we will detail only the specifics of ADMIRE relevant to the iterative variant.

The physical model is denoted by X, and is comprised of model predictors for the region of interest $X_{\rm ROI}$ and model predictors for other sources $X_{\rm clutter}$. Using this model, we have

$$y = X\beta, \tag{4}$$

where y is the post-short-time Fourier Transform (STFT) aperture signal for a single frequency at a given depth, and β is the set of model coefficients for the model predictors. Since the size of the model is vastly larger than the aperture signal making (4) inherently ill-posed, we must solve for the model coefficients using elastic-net regularization [9], by the equation

$$\hat{\beta} = \arg\min_{\beta} (||y - X\beta||^2 + \lambda(\alpha||\beta||_1 + (1 - \alpha)||\beta||_2^2)), \quad (5)$$

where $||\beta||_1$ is the L1 norm, $||\beta||_2$ is the L2 norm, α is a weighting between the L1 and L2 norms, and λ is a regularization parameter that corresponds to the degrees of freedom [10]. For this study, we set $\alpha = 0.9$, and chose λ for a high degree of freedom.

Once the model coefficients have been estimated from the elastic-net regularization, we can estimate the decluttered, frequency-domain aperture signal by selecting exclusively the model predictors sampled from the region of interest as

$$y_{\text{decluttered}} = X_{\text{ROI}} \hat{\beta}_{\text{ROI}},$$
 (6)

and further we can take the inverse short-time Fourier Transform to get the time-domain signal.

E. Iterative ADMIRE (iADMIRE)

Iterative ADMIRE (iADMIRE) extends ADMIRE to iteratively solve for the model predictors in the elastic-net regularization step, theoretically producing a more accurate estimation of the region of interest signal. Algorithm 1 details the steps for iteratively calculating and removing clutter.

For every iteration, we start by calculating the model coefficients $\hat{\beta}_k$ using (5). Since the physical model is split into region of interest and clutter predictors, we can estimate the clutter-only signal using (7). We can then update the aperture signal by subtracting the clutter-only signal, until eventually the difference between signal iterations is smaller than some predetermined threshold. At this point, the decluttered signal is calculated with (6) using the most recent set of model coefficients. This overall process helps to eliminate strong

sidelobe clutter, producing a more accurate region of interest signal.

III. METHODS

A. Contrast Target Phantom

For measuring the dynamic range, we used Field II [11], [12], where we simulated 5 mm diameter cysts of known contrast from -50 dB to 70 dB relative to the background, plus a 90 dB and anechoic case. For each level of contrast, 12 realizations of speckle were created. Reference [1] includes more details about the simulation parameters. We prefer this method of measuring dynamic range as it allows us to evaluate the methods at sharp changes in contrast.

B. Bright Scatterer Phantom

For measuring the effect on the DRA, we again used Field II to simulate single point targets with contrasts from 40 dB to 120 dB relative to the background. For each level of contrast, 6 realizations of speckle were created. The same Field II parameters were used as for the contrast target phantoms.

C. Contrast and Dynamic Range

For both simulation cases, the contrast ratio was defined as

$$CR = 20 \log_{10}(\frac{\mu_{\text{ROI}}}{\mu_{\text{background}}}),$$
 (9)

where μ is the mean value of the enveloped, pre-compression data. The background corresponds to a region of pure background speckle for both simulation cases. For the contrast target phantoms, the ROI corresponds to the 5 mm cyst, but for the bright scatterer phantoms it corresponds to an area where the dark region artifact is present. Finally, a two-tailed t-test ($\alpha = 0.05$) was used to statistically determine the point at which each method deviated from the true contrast, which is the dynamic range.

Algorithm 1: Iterative clutter removal in ADMIRE

- 1 Given model predictors $X = [X_{ROI} \ X_{clutter}]$, aperture signal y_1 , parameters α and λ , and $\delta > 0$
- **2 for** k = 1 **do**
- 3 Solve (5) for model coefficients $\hat{\beta}_k$, given y_k , X
- 4 Compute clutter-only signal

$$y_{k,\text{clutter}} = X_{\text{clutter}} \hat{\beta}_{k,\text{clutter}}$$
 (7)

5 Compute new aperture signal

$$y_{k+1} = y_k - y_{k,\text{clutter}} \tag{8}$$

- 6 Stop when $||y_{k+1} y_k||_2^2 < \delta$
- 7 end for
- 8 Calculate $y_{\text{decluttered}} = X_{\text{ROI}} \hat{\beta}_{k,\text{ROI}}$

IV. RESULTS

Fig. 1 (top) reports the estimated contrast ratio dynamic range for each beamformer, while (bottom) shows the measured contrast for each contrast phantom compared to the true contrast from anechoic to 90 dB. In this study, DAS has an impressive range of 50.4 dB, which is just slightly better than ADMIRE at 49.3 dB. iADMIRE manages a significant improvement over both methods with range of 69.6 dB. DMAS and GCF both have greatly reduced range compared to DAS. It is important to note here that the parameters for the physical model creation in ADMIRE can be tuned to significantly different results. In particular, in our previous study ADMIRE performed slightly better than DAS [6], but for this study the parameters were tuned more for DRA removal.

An example set of bright scatterer phantom images is shown in Fig. 2. The contrast of the dark artifact region is calculated from the solid and dashed red lines for all cases. The contrast in DAS of 3.23 dB is slightly greater than 0 due to focusing and the difference in depths of the regions. The DRA is the most prevalent in GCF and ADMIRE, with the severity increasing as the contrast of the target increases. DMAS also experiences the DRA at higher levels, though it is very slight comparatively. In comparison, DAS and iADMIRE have no DRA present, though DAS instead exhibits strong distortion of the background speckle in those areas at 100 dB and above. iADMIRE is able to reduce the DRA and additionally suppress sidelobes and fully preserve the speckle texture in cases up to 100 dB, though in acoustically stronger cases the speckle began to distort as well. In the 100 dB case where the improvement was the most significant, the contrast of the DRA was 4.56 ± 0.61 dB for DAS, -5.02 ± 1.26 dB for DMAS, -20.67 ± 0.72 dB for GCF, -24.43 ± 0.62 dB for ADMIRE, and -0.58 ± 0.84 dB for iADMIRE.

V. DISCUSSION AND CONCLUSIONS

In this study we introduced iterative ADMIRE, an extension of ADMIRE specifically aimed at increasing its dynamic range and mitigating dark region artifacts. We showed that iADMIRE is able to attain a dynamic range of 69.6 dB, an improvement of 19.2 dB compared to DAS and 20.3 dB compared to ADMIRE. Additionally, we showed that iADMIRE was able to mitigate the DRA and fully preserve the speckle texture in bright scatterer cases up to 100 dB, while also suppressing sidelobes compared to DAS.

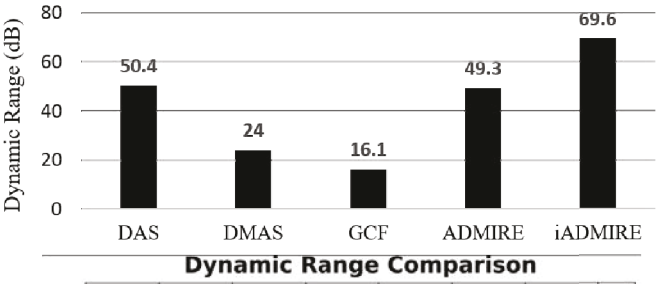
ACKNOWLEDGMENT

The authors would like to thank the staff of the Vanderbilt University ACCRE computing resource. This work was supported by NIH grants R01EB020040 and S10OD016216-01, and additionally by NSF award IIS-1750994.

REFERENCES

[1] K. Dei, A. Luchies, and B. Byram, Contrast ratio dynamic range: a new beamformer metric, IEEE International Ultrasonics Symposium (IUS), pp. 1-4, September 2017.

Contrast Dynamic Range



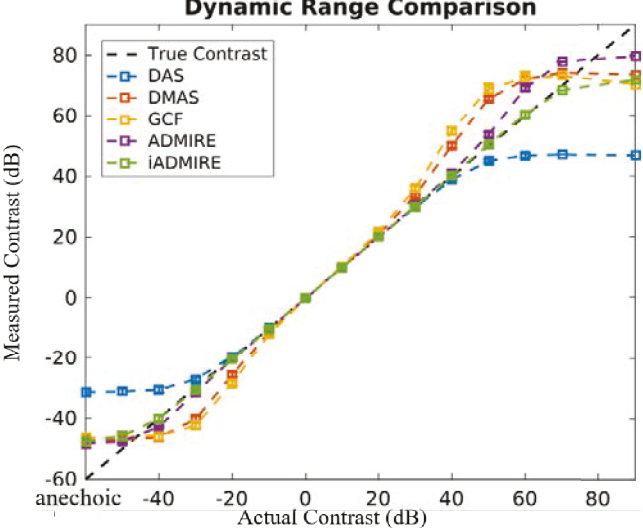


Fig. 1. The estimated contrast ratio dynamic range (top) and measured contrast (bottom) for each tested beamformer. iADMIRE performs the best, with an improvement of 19.2 dB compared to DAS. ADMIRE has nearly as much dynamic range as DAS, but DMAS and GCF both have significantly less range.

- [2] O.M.H. Rindal, A. Rodriguez-Molares, and A. Austeng, The Dark Region Artifact in Adaptive Ultrasound Beamforming, IEEE International Ultrasonics Symposium (IUS), September 2017.
- [3] B. Byram, K. Dei, J. Tierney, and D. Dumont, A model and regularization scheme for ultrasonic beamforming and clutter reduction, IEEE Transactions on Ultrasonics, Ferroeletrics, and Frequency Control, vol. 62, no. 11, pp. 1913-1927, 2015.
- [4] K. Dei and B. Byram, The impact of model-based clutter suppression on cluttered, aberrated wavefronts, IEEE Transactions on Ultrasonics, Ferroeletrics, and Frequency Control, 2017.
- [5] B. Byram and M. Jakovljevic, "Ultrasonic multipath and beamforming clutter reduction: a chirp model approach," IEEE Transactions on Ultrasonics, Ferroeletrics, and Frequency Control, vol. 61, no. 3, pp. 428-440, 2014.
- [6] K. Dei and B. Byram, A Robust Method for Ultrasound Beamforming in the Presence of Off-Axis Clutter and Sound Speed Variation, Ultrasonics, vol. 89, pp. 34-45, September 2018.
- [7] G. Matrone, A.S. Savoia, G. Caliano, S. Member, and G. Magenes, "The Delay Multiply and Sum Beamforming Algorithm in Ultrasound B - Mode Medical Imaging", IEEE Trans. Med. Imaging, vol. 34, no. 4, pp. 1-10, 2015.
- [8] P. C. Li and M. Li, Adaptive imaging using the generalized coherence factor, IEEE Transactions on Ultrasonics, Ferroeletrics, and Frequency Control, vol. 50, no. 2, pp. 128-141, 2003.
- [9] H. Zou and T. Hastie, Regularization and variable selection via the elastic net, Journal of the Royal Statistical Society: Series B (Statistically Methodology), vol. 67, no. 2, pp. 301-320, 2005.
- [10] R. J. Tibshirani, J. Taylor et al., Degrees of freedom in lasso problems, The Annals of Statistics, vol. 40, no. 2, pp. 1198-1232, 2012.

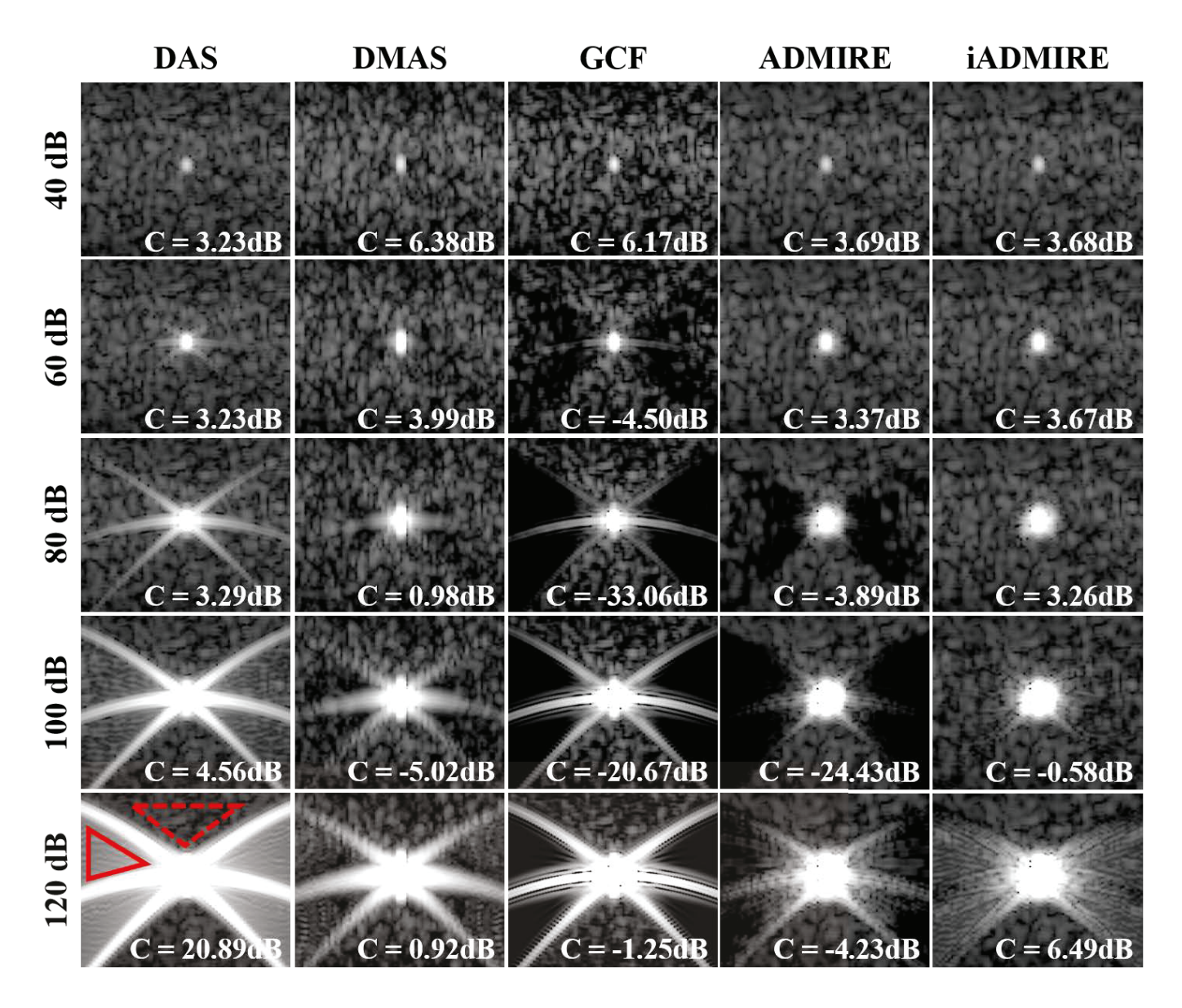


Fig. 2. Bright scatterer phantom images for tested beamformers presented with a dynamic range of 60 dB. The dark region artifact (DRA) appears most significantly in GCF and ADMIRE, and appears slightly in DMAS. iADMIRE greatly reduces the DRA compared to normal ADMIRE, preserving underlying speckle texture in cases up to 100 dB. DAS does not experience a DRA, but the speckle is still distorted in cases at or above 100 dB. In the bottom left image, the solid red line indicates the DRA and the dashed red line indicates the background used for contrast measurements. The contrast listed is the average contrast of the DRA relative to the background across all six realizations.

- [11] J.A. Jensen, Field: A Program for Simulating Ultrasound Systems, Paper presented at the 10th Nordic-Baltic Conference on Biomedical Imaging Published in Medical & Biological Engineering and Computing, vol. 34, supplement 1, part 1, pp. 351-353, 1996.
- [12] J.A. Jensen and N.B. Svendsen, Calculation of pressure fields from arbitrarily shaped, apodized, and excited ultrasound transducers, IEEE Transactions on Ultrasonics, Ferroeletrics, and Frequency Control, vol. 39, pp. 262-267, 1992.